Pulmonary administration of a dry powder formulation of the antifibrotic drug tilorone reduces silica-induced lung fibrosis in mice

Ville Vartiainen, Janne Raula, Luis M. Bimbo, Jenni Viinamäki, Janne T. Backman, Nurcin Ugur, Esko Kauppinen, Eva Sutinen, Emmi Joensuu, Katri Koli, Marjukka Myllärniemi

PII: S0378-5173(18)30232-1
DOI: https://doi.org/10.1016/j.ijpharm.2018.04.019
Reference: IJP 17426

To appear in: *International Journal of Pharmaceutics*

Received Date: 14 January 2018
Revised Date: 9 April 2018
Accepted Date: 10 April 2018

Please cite this article as: V. Vartiainen, J. Raula, L.M. Bimbo, J. Viinamäki, J.T. Backman, N. Ugur, E. Kauppinen, E. Sutinen, E. Joensuu, K. Koli, M. Myllärniemi, Pulmonary administration of a dry powder formulation of the antifibrotic drug tilorone reduces silica-induced lung fibrosis in mice, *International Journal of Pharmaceutics* (2018), doi: https://doi.org/10.1016/j.ijpharm.2018.04.019

Pulmonary administration of a dry powder formulation of the antifibrotic drug tilorone reduces silica-induced lung fibrosis in mice

Ville Vartiainen[a,c,*], Janne Raula[b], Luis M. Bimbo[e], Jenni Viinamäki[f], Janne T. Backman[f], Nurcin Ugur[b], Esko Kauppinen[b], Eva Sutinen[a], Emmi Joensuu[c], Katri Koli[c,†] and Marjukka Myllärniemi[d, †]

[a] Department of Clinical Medicine, Division of Pulmonary Medicine, University of Helsinki, Finland

[b] Department of Applied Physics, Aalto University School of Science, Finland

[c] Research Programs Unit, Translational Cancer Biology, University of Helsinki, Finland

[d] University of Helsinki and Helsinki University Hospital, Heart and Lung Center and HUH Diagnostics, Pulmonary Medicine, Finland

[e] Strathclyde Institute of Pharmacy and Biomedical Sciences, University of Strathclyde, United Kingdom, and Division of Pharmaceutical Chemistry and Technology, Faculty of Pharmacy, University of Helsinki, Finland

[f] Department of Clinical Pharmacology, University of Helsinki and Helsinki University Hospital, Finland

† These authors contributed equally

***Corresponding author**: Ville Vartiainen, Haartmaninkatu 3, 00014 Helsinki, Finland, Phone +358504306414, E-mail ville.vartiainen@helsinki.fi

Keywords: idiopathic pulmonary fibrosis, antifibrotics, tilorone, dry powder inhaler

Abstract

The aim of this work was to study the antifibrotic effect of pulmonary administration of tilorone to lung fibrosis. L-leucine coated tilorone particles were prepared and their aerosolization properties were analyzed using two dry powder inhalers (Easyhaler and Twister). In addition, the biological activity and cell monolayer permeation was tested. The antifibrotic effect of tilorone delivered by oropharyngeal aspiration was studied *in vivo* using a silica-induced model of pulmonary fibrosis in mice in a **preventive setting.** When delivered from the Easyhaler in an inhalation simulator, the emitted dose and fine particle fraction were independent from the pressure applied and showed dose repeatability. However, with Twister the **aerosolization** was pressure-dependent indicating poor compatibility between the device and the formulation. The formulation showed more consistent permeation through a **differentiated Calu-3** cell monolayer compared to pristine tilorone. Tilorone decreased the histological fibrosis score *in vivo* in systemic and local administration, but only systemic administration decreased the mRNA expression of type I collagen. The difference was hypothesized to result from 40-fold higher drug concentration in tissue samples in the systemic administration group. These results show that tilorone can be formulated as inhalable dry powder and has potential as an oral and inhalable antifibrotic drug.

1. Introduction

Idiopathic pulmonary fibrosis (IPF) is a severe progressive lung disease with poor prognosis. The median survival is 2 to 7 years from diagnosis and comparable to many malignant disorders (18, 37). There are two drugs in clinical use, pirfenidone and nintedanib, which can be used to slow down disease progression. Both drugs are new, expensive, and have a somewhat difficult adverse effect profile. In phase 3 clinical trials, over 90% of the patients reported at least one adverse effect (18, 37). Adverse effects of nintedanib are mainly GI-tract related e.g. nausea and diarrhea, while pirfenidone shows also skin related adverse effects e.g. phototoxicity and rash. Reports from recent real-life studies confirm the adverse effect profiles of these drugs on a population level (3, 6, 16).

Tilorone is an old anti-viral drug which has been characterized as an interferon inducer (39). However, it also shows therapeutic effects that are independent of interferon induction (9, 39). Tilorone inhibits transforming growth factor β (TGF-β) signaling pathway (23), which has been shown to be upregulated in fibrotic lungs (2). Lung tissue of IPF patients also shown increased levels of the bone morphogenetic protein (BMP) inhibitor gremlin-1 (19). Rescue of BMP signaling, by administration of BMP-7, is antifibrotic in *in vivo* mouse models (24, 29). Tilorone has been shown to induce BMP signaling and act as an antifibrotic agent *in vivo* in a mouse model of pulmonary fibrosis (23).

Local administration of drugs directly into the lungs is hypothesized to result in decreased adverse effects and cost. As the drug is only administered to the affected organ, it would likely lead to lower total doses and result in decreased systemic exposure. For example, the dose of inhaled corticosteroids in modern asthma treatment is only a fraction of the dose used in oral administration (1). This has enabled the long term use of a drug class that otherwise would have

elicited severe adverse effects by systemic dosing. Pulmonary administration has been studied and proposed also for the currently used IPF drug pirfenidone (12, 30, 38, 43) and N-acetylcysteine (7, 31).

Previously we have developed a method, the aerosol flow reactor method, which has been successfully employed for particle production of both freely and poorly water-soluble drugs and their combinations as carrier free inhalable dry powders (34, 40, 41). It is a one-step continuous process to simultaneously produce, encapsulate, and coat drug particles resulting in highly flowable and dispersible dry powders. Particles are encapsulated and coated with the amino acid L-leucine producing two qualitatively different L-leucine layers. The encapsulation formed *via* leucine diffusion to the particle's surface (10, 27) protects the drug from moisture (36). The coating, which is formed *via* the physical vapor deposition of leucine, is composed of nano-sized crystals of leucine to form a rough coating. These nanocrystals allow firstly, the spatial separation of the particles and secondly, a reduction of the contact area to lower adhesion forces between particles and surfaces (32). These properties are imperative for good dispersion properties of dry powders (34).

The aim of this work was to promote the therapeutic potential of tilorone, a known antifibrotic small molecule, *via* the lungs using dry powder inhalation (DPI) delivery. For this, we prepared L-leucine coated tilorone dry particles, which were analyzed for their aerosolization properties, cell permeation and *in vitro* activity. Finally, the antifibrotic effect of tilorone in pulmonary administration was studied in a mouse model of silica-induced fibrosis.

2. Materials and methods

2.1. Preparation of the aerosol nanoparticles

Tilorone (5 g/L, Hangzhou Pharma & Chem), D-mannitol (10 g/L, Alfa Aesar) and L-leucine (10 g/L, Alfa Aesar) were dissolved in deionized water to produce a precursor solution for the aerosol processing. The aerosol flow reactor method has been discussed in detail in previous studies (8, 26, 33). Briefly, the solute droplets were generated by an ultrasonic nebulizer (RBI Pyrosol 7901) and transferred with nitrogen gas (20 L/min) to the stainless steel aerosol reactor **(diameter 100 mm and length 1800 mm)** where temperature was set to 180 °C (± 1 °C). **As a surface active agent, L-leucine accumulated in the air-liquid interface from where it was sublimated by the reactor's temperature.(10, 27) This process generated a cloud of L-leucine around the particles.** At the reactor downstream, the aerosol was rapidly diluted and cooled with a large volume of pressurized air (22 °C, 80 L/min; Reynolds number > 3000) in a porous stainless steel tube to avoid the wall deposition of particles and to initiate nucleation and deposition of leucine vapor on drug particle surfaces. **The aerosol flow were then lead to a small-scale cyclone (height 85 mm, body diameter 35 mm, exit tube length 45 mm, and exit and inlet tube diameter 10 mm) where the solid aerosol particles were collected (45).**

2.2. Particle morphology

The particle morphology was studied with field-emission scanning electron microscope (Zeiss Sigma VP) with acceleration voltage of 2 kV. The samples were coated with sputtered platinum to enhance image contrast and to stabilize the particles under the electron beam.

2.3. Analysis of powder composition

The composition of the powder was determined using proton nuclear magnetic resonance spectrometry (1H-NMR) (Bruker AVANCE 400 MHz) in D_2O. Chemical shifts used were for tilorone: δ = 1.2 ppm (6H), L-Leucine: δ = 1.6 ppm (3H) and D-Mannitol δ = 4.5 ppm (2H).

2.4. Powder aerosolization

All the fine powders were stored in a desiccator over silica gel (0–1% of relative humidity) prior to the inhalation experiments. The aerosolization of the carrier-free powders was studied using a computer-assisted inhalation device developed in-house. Its detailed operating principles have been discussed elsewhere (17, 20) and its applicability for the aerosolization of powders has been demonstrated (20, 34). Briefly, the inhalation profile is created through interplay between a vacuum and pressurized air gas by a controlled valve system **(see supplementary Fig. 1)**. **The low pressure impactors require stable flow to accurately sort the particles according to their aerodynamic diameter. In between the actuations, the device is fed by a bypassed flow to ensure constant mass flow to the analysis instrumentation while giving zero net flow to the mouth piece of the inhaler. The bypassed flow is led to the instrument through a porous metal tube to create a particle-free film on the edge of the flow. When the actuation is initiated, the controlled valve system diverts part of the bypassed flow to the inhaler mouth piece resulting in emission of the powder. The laminar particle free flow on the surface of the tubing prevents particle collision with the tubing and therefore ensures that the particle agglomerates are not broken by the instrument after they leave the inhaler.**

Two inhalers, multi-dose reservoir-type Easyhaler inhaler (Orion Pharma) and single-dose capsule Twister inhaler (Aptar Pharma), were used. The Easyhaler reservoir was filled with approx. 0.8 g of fine drug powder, and the hydroxypropyl methylcellulose (HPMC) capsules (Vcaps size 3, Capsugel)

used in Twister were filled with 5.0 ± 0.1 mg/capsule of fine drug powder. Doses to the inhalers were conveyed as instructed by the providers. Prior to the actual inhalation experiments, five powder doses were run and discarded. Powder emission (emitted dose, ED, 10 repetitions) was detected gravimetrically by weighing the inhaler or inhaler and capsule before and after each inhalation. Pressure drops over the inhalers were adjusted to 2 and 4 kPa corresponding to the inspiration flow rates of 40 L/min and 55 L/min for Easyhaler and 43 L/min and 55 L/min for Twister. The inhalation profiles were fast, *i.e.*, the maximum pressure drops and flow rates were achieved in two seconds maintaining these sets for 8 s and then stopped. Fine particle fractions (FPF, the fraction of particles with the geometric number mean diameter (D_g) size less than 5.5 μm) were measured gravimetrically on collection stages of a Berner-type low pressure impactor (BLPI) (15). The dispersed fine particles were collected isokinetically by the BLPI (15) with a stage aerodynamic cut-off diameters ranging from 0.03 to 15.61 μm. Mass median aerodynamic diameters (MMAD) and related geometric standard deviations (GSD) of the deposited powders were determined by

$$MMAD = \exp\left(\frac{\sum(m_i \ln D_i)}{M}\right)$$

$$GSD = \exp\left(\left(\frac{\sum\left(m_i D_i^3 (\ln D_i - \ln MMAD)\right)^2}{\sum(m_i D_i^3) - 1}\right)^{1/2}\right)$$

respectively, where m_i is the mass fraction of particles on the collection stage, D_i is the mean aerodynamical diameter of the particles at the collection stage, and M is the sum of mass fractions and

is, by definition, unity. Fine particle fractions (FPF, $D_g \leq 5.5$ μm) were expressed with reference to the emitted dose (ED).

2.5. Cell culture

Calu-3 (HTB-55) human airway epithelial cells were obtained from American Type Culture Collection (ATCC). Cells from passages 35–38 were used in the experiments. TGF-β [$(CAGA)_{12}$-luc] and BMP [$(Bre)_2$-luc] pathway reporter cell lines (A549 lung adenocarcinoma cells, CCL-185, ATCC) were produced as described elsewhere (23). The cells were cultured in Dulbecco's Modified Eagle's Medium (DMEM, HyClone) supplemented with 10% FBS, 1% L-glutamine, 100 IU/ml penicillin, 100 μg/ml streptomycin (all from HyClone). Reporter cell lines were cultured in the presence of 0.4 mg/ml G418 (Sigma-Aldrich). The cultures were maintained in a MCO 170-M multi-gas incubator at 37°C (Panasonic Biomedical) in an atmosphere of 5% CO_2 and 95% relative humidity. The growth medium was changed three times per week.

2.6. *In vitro* drug permeation

The permeability of tilorone powder (formulated or unprocessed) across a differentiated Calu-3 lung cell monolayer was measured as described elsewhere (40). Briefly, cells were seeded into Transwell inserts (0.4 μm pores size, surface area of 1.12 cm^2, Costar) at a density of 5×10^5 cells/cm^2. To promote the differentiation of the Calu-3 cells, an air-liquid interface was induced by removing the media from the apical side 24 h after seeding. The cells were then allowed to differentiate for 14–22 days. The integrity of the Calu-3 cell monolayer and tight junction barrier function were assessed before and after the permeation experiment by measuring the transepithelial electrical resistance (TEER) using a Millicell Electrical Resistance System (Millipore). Before the deposition experiment, the medium from the basolateral compartment was replaced with fresh PBS. Afterwards, 10 μL of Curosurf lung

surfactant (Chiesi Farmaceutici) which contains polar lipids, in particular dipalmitoylphosphatidylcholine (DPPC, ~50% of the total phospholipid content), was gently pipetted on top of the cell monolayer in the apical compartment. Subsequently, approximately 2 mg of the formulated tilorone or 1 mg of unprocessed tilorone was deposited in each of the wells. The samples were collected over a period of 180 min by sampling 500 μL from the basolateral compartment and replacing the taken volume with fresh PBS.

The tilorone concentration in the samples was determined using a Hewlett Packard series 1100 liquid chromatography system (Hewlett Packard) with ultraviolet detection (λ = 273 nm). The chromatographic separation was performed on a Kinetex EVO C18 column (2.6 μm particle size, inner diameter 4.6 mm × 150 mm, Phenomenex).

The mobile phase consisted of 100 mM formic acid in water (A), and acetonitrile (B) in an 82:18% v/v ratio (isocratic run, total run time 6 min). The mobile phase flow rate was set at 700 μL/min and the injection volume was 10 μL. The amount of permeated tilorone was calculated in relation to the original drug amount present in the dry powder particles. The results are the averages of four independent experiments

2.7. TGF-β/BMP luciferase reporter assays

TGF-β [$(CAGA)_{12}$-luc] or BMP [$(Bre)_2$-luc] pathway reporter cells were seeded into 96-well plates ($1.5\text{-}2\times10^4$/well) and allowed to attach for 5 hours. Stimulation media containing 5% FBS and different concentrations of tilorone powders were added to the cells. TGF-β (0.5 ng/ml) or BMP-4 (5 ng/ml) was used as a positive control. Cells were stimulated for 18h after which they were lysed and subjected to luciferase activity measurements using the Luciferase Assay System (Promega) measured with DCR-1

luminometer (MGM Instruments) as previously described (23). Three independent assays were performed.

2.8. *In vivo* mouse model of pulmonary fibrosis

Experiments involving mice were approved by the Finnish national animal experiment board (ESAVI/10418/04.10.07/2016) and carried out in accordance with institutional guidelines, which fulfill the requirements defined in regulations of the Finnish Act on the Protection of Animals used for Scientific or Educational Purposes (497/2013) and were performed according to the 3R.

To induce pulmonary fibrosis, a modified version of the method described by Lakatos *et al.* was used (22). Male C57b6/J mice (Envigo) were exposed to silicon dioxide (SiO_2, 50 mg/kg in 50 µL PBS, Sigma-Aldrich) by two subsequent oropharyngeal aspiration doses on days 1 and 5 as previously described (23). The mice were treated with tilorone three times a week for three weeks starting on day 1. For systemic administration, the mice were given tilorone (50 mg/kg) by intraperitoneal injection. For pulmonary administration, the tilorone formulation was dissolved in sterile PBS and administered by oropharyngeal aspiration (tilorone dose 5 mg/kg). The vehicle group (pulmonary administration) received excipients (L-leucine and D-mannitol) dissolved in sterile PBS at same doses as the group receiving the tilorone formulation.

All mice were sacrificed on experiment day 22. The entire left lung was fixed in 4% paraformaldehyde and embedded in paraffin. The right lung was snap frozen in liquid nitrogen and stored at -70 °C. To produce homogenous lung tissue powder for subsequent analyses, the right lung was crushed with mortar and pestle under liquid nitrogen.

2.9. Histological analyses

Lung tissue sections (3 μm) were stained with hematoxylin and eosin for histological evaluation. The degree of pulmonary fibrosis and inflammation was evaluated using a semi-quantitative scale from 0-3 allowing half steps. The scoring was performed by two blinded researchers and in case of disagreement the scoring was discussed until consensus was found. For the histological micrographs the slides were scanned digitally (Pannoramic FLASH II, 3DHistech) and analyzed using CaseViewer program (3DHistech).

2.10. RNA isolation and quantitative RT-PCR

Total lung tissue RNA was isolated with RNeasy Mini Kit (Qiagen) and RNA integrity was analyzed using TapeStation (Agilent Technologies) at the Biomedicum Functional Genomics Unit (HiLife, Helsinki). Complementary DNA was synthesized with iScript cDNA Synthesis Kit (BioRad). The cDNAs were amplified using TaqMan Assays-on-Demand gene expression products (Applied Biosystems) and CFX96 Real-time PCR detection system (Bio-Rad). The relative gene expression differences were calculated with the comparative ΔΔCT method and the results have been expressed as mRNA expression levels normalized to the levels of a gene with a constant expression (TBP, TATA-binding protein).

2.11. Analyses of drug tissue concentrations

The lung samples were processed according to the procedure by Zhang *et al* (44).The homogenized tissue samples were weighed and purified water was added to reach a final volume of 200 μl. Calibration samples were prepared in human plasma. Metoprolol (Toronto Research Chemicals) was used as an internal standard. The drug concentrations were determined by using a Shimadzu Nexera

liquid chromatography system (Shimadzu Corporation) coupled to a Shimadzu Nexera 8050 tandem mass spectrometer (Shimadzu Corporation). The chromatographic separation was performed on Waters XBridge C18 column (3.5 µm particle size, inner diameter 2.1 mm x 100 mm, Waters Corporation) equipped with Waters XBridge C18 pre-column. The mobile phase consisted of 10 mM ammonium acetate in water (pH 9.5) (A) and methanol (B) (gradient separation, 5-100% B, total run time 7 min). The mobile phase flow was set at 300 µl/min and the injection volume was 10 µl. The mass spectrometry detection was performed using electro-spray ionization in positive mode and monitoring multiple reactions of the $[M+NH_4]^+$ (tilorone) or $[M+H]^+$ (metoprolol) precursor ions to the product ions for analyte and internal standard as follows: m/z 427 –>86 for tilorone, and 268 –> 116 m/z for metoprolol. The lower limit of quantification (LLOQ) was 1 ng/ml and day-to-day repeatability 12.8%.

2.12. Statistical analysis

The numerical data are presented as the mean ± standard deviation (SD). Data from activity and *in vivo* -experiments were analyzed for statistical significance with nonparametric Mann-Whitney test using SPSS Statistics 24 software (IBM). For the permeation experiment, a multiple t-test followed by a Holm-Šídák correction test (significance level, alpha, set to 5%) was used to compare all individual data points. P-values less than 0.05 were considered significant.

3. Results

3.1. Particle morphology and composition

We first attempted to produce tilorone dry powder with leucine as the only excipient. This was not successful as the particles strongly agglomerated and aggregated showing cuboid rather than spherical morphology upon collection by cyclone (**Supplementary Fig. 2**). It is likely that tilorone did not

crystallize upon particle formation but remained in an amorphous state in the particles. However, once collected tilorone started to crystallize resulting in sintered, aggregated particles. Sintering prevents the dispersion of the produced single particles upon inhaler actuation, resulting in aerosolized aggregates that are too large for deep lung deposition. The excipient mannitol was added as a reinforcing matrix component to reduce or even prevent the sintering by dilution. It has been shown that mannitol crystallizes in the aerosol particle production (21) . Being more stable than amorphous, the crystalline state is more resistant to phase changes in both collection and storage. Addition of mannitol resulted in stable particle morphology and particle agglomeration was avoided.

The powder formulation contained 29.4 m-% of tilorone, 9.6 m-% of leucine and 61.0 m% of mannitol as determined by proton-NMR (**NMR spectrum in supplementary Fig. 3**). The SEM micrograph of tilorone dry powder (Fig. 1) shows spherical particles with the rough leucine coating. Some aggregation is observed with the larger particles, which could be real agglomeration or an artefact formed during sample preparation for the SEM.

3.2. Powder aerosolization

To allow reliable dosing despite age, gender, or clinical state of the patient, the dry powder formulation needs to aerosolize and disperse in a pressure and flow rate-independent manner. Tilorone dry powder showed good aerosolization characteristics especially when delivered from the Easyhaler inhaler (Table 1). In case of applying Easyhaler, the ED and FPF showed virtually no pressure dependence. Dose repeatability in the ED described by CV_{ED} was well within acceptable limits, being under 10 % for both pressure drops. However, when delivered from the Twister inhaler the aerosolization performance of the tilorone powder was more dependent on the applied pressure drop. At 2 kPa, the ED was 17 % higher and the FPF was 33 % lower than the corresponding results carried out at 4 kPa. These

differences could lead to clinically significant variation in dosing depending on the clinical state of the patient. Dose repeatabilities (CV_{ED}) for the ED were acceptable, but showed some variation as function of pressure drop.

3.3. Biological activity of the formulation *in vitro*

The aerosol flow reactor method involves heating of the drug up to 180 °C during droplet drying and leucine sublimation process. Since many chemical compounds are unstable at such temperatures, we studied the biological activity of the tilorone formulation in an *in vitro* setting. The activity was analyzed using two luciferase reporter assays (see Methods). We have previously shown that tilorone decreases TGF-β and increases BMP signaling activity in lung epithelial cells (23) . The formulation showed a concentration dependent response in both inhibition of TGF-β signaling and induction of BMP signaling suggesting retained biological activity (Fig. 2). Also, there was no statistically significant difference in the activity of the formulation when compared to its pristine counterpart at equal tilorone doses.

3.4. Cell monolayer powder permeation *in vitro*

Effective DPI formulations require the powder to adhere onto the lung walls in order to allow drug molecules to permeate the pulmonary epithelium or at least become freely available for absorption in the lung parenchyma in order to achieve a therapeutic effect (13, 14). The permeability of formulated and unprocessed tilorone powders was measured across a differentiated Calu-3 lung cell monolayer in the apical to basolateral direction. The TEER was measured before and after the experiments to assert monolayer integrity. The average value obtained for all the wells before the deposition was 514 ± 39 Ωcm^2, which is in good agreement with values reported in the literature (14) . However, a sharp decline in TEER values (over 37%) was registered after the experiment, which is likely to be related to the

introduction of the Curosurf surfactant in the apical compartment. Curosurf contains roughly 50% DPPC, a phospholipid known to substantially decrease TEER values of Calu-3 differentiated cell monolayers therefore allowing increased drug permeation (4) . In the case of unprocessed tilorone 17.6 % of the deposited drug was able to permeate through Calu-3 cell monolayer, whereas only 11.2 % of the formulated tilorone permeated (Fig. 3). The differences were found not to be statistically significant. However, the formulated powder showed less variation and therefore, more consistent permeation.

3.5. Pulmonary administration of tilorone *in vivo*

The antifibrotic activity of tilorone delivered using pulmonary administration was studied using a silica-induced pulmonary fibrosis model in mice. The mice were divided into four groups (n=12) upon arrival; the first group was assigned as control and did not receive fibrosis induction or any treatment (non-treated), the second group was exposed to silica and received only excipients (mannitol and leucine) through aspiration (SiO_2-ctrl), the third group was exposed to silica and received tilorone through intraperitoneal injection (SiO_2-systemic) and the fourth group was exposed to silica and received dissolved tilorone microparticles through aspiration (SiO_2-local). Mice exposed to silica suffered a weight loss of 1-2 g after both silica exposures (Supplementary Fig 4). Otherwise there were no observable adverse effects due to silica exposure or pulmonary administration. There was no observed mortality during the experiment in any of the groups.

Histological analyses of lung tissue indicated that both systemically and locally administered tilorone decreased fibrotic alterations (Fig 4A). In agreement with our previous reports (23), histological scoring indicated that systemic administration of tilorone significantly decreased fibrosis ($p=0.013$) and inflammation ($p=0.010$) in fibrotic mice (Fig. 4B). Local dosing also resulted in a significantly lower

fibrosis score (p=0.028). However, the inflammation score showed only a non-significant decrease in the locally treated group (p=0.103).

To analyze the effect of locally administered tilorone on pulmonary parenchyma matrix deposition, the mRNA expression of type I collagen (*Col1a1*) was measured from homogenized lung tissue samples. *Col1a1* expression increased in response to SiO_2-exposure and was reversed by systemic tilorone administration (Fig. 5, p=0.010). Local dosing had no effect on *Col1a1* expression.

To assess the pharmacokinetic properties of tilorone in pulmonary administration, tilorone concentrations were measured from the homogenized lung tissue samples. The non-treated and control groups did not receive tilorone and no tilorone could be detected in these groups, as expected. For the systemic administration group the tilorone content was 507.4±50.5 μg/ml and for the local administration group, it was 12.1±1.2 μg/ml.

4. Discussion

Effective drug delivery to the lung parenchyma can be achieved by a well-performing inhalation product that is correctly administered to the patient. One of the inhalation platforms is dry powder, where micronized drug particles with size < 5 μm, suitable for delivery to alveolar region, (42) are delivered from DPI inhalers. These particles, however, are usually very cohesive (28) resulting in poor flowability and dispersibility. This is why the particles are usually blended with coarser carrier particles to ensure dose repeatability upon inhalation. Particle engineering plays an important role in the fabrication of carrier-free formulations with accurate dosing and delivery properties. Our carrier-free

tilorone formulation showed pressure independent behavior especially with Easyhaler. The **tilorone formulation shows somewhat lower FPF than our previous leucine-based formulations with corticosteroids or corticosteroid-β-agonist combination.**(35, 40, 41) **However, ED and CV are well in line with our previous formulations. It is possible, that the presented tilorone formulation is suboptimal and could further be improved by addition of excipients or careful adjustment of the L-leucine saturation conditions.**

As tilorone is a freely water-soluble compound, drug solubility is not a significant bottleneck for its *in vivo* administration and biodistribution. However, as the unprocessed tilorone powder has unequal particle size it is likely to produce uneven permeation profiles leading to potential dose-dumping effects. By formulating tilorone as a DPI, which enables precise control over drug content, particle size, and morphology, it is possible to achieve more reproducible drug release profiles. The presented results highlight the value of processing even freely water-soluble compounds as DPIs, where precise control over are particle size and drug dosing play a critical role for clinical translation.

While the mechanism of action of the oral antifibrotic agent pirfenidone is not completely understood, it has been shown to prevent TGF-β induced proliferation and fibrogenic activity of primary human lung fibroblasts and human Tenon's fibroblasts *in vitro* (5, 25). Therefore, it seems to share at least one common pathway with tilorone. Pulmonary formulations of pirfenidone have been studied in both *in vitro* and *in vivo*. Seto *et al.* (38) studied the pharmacokinetic profile of spray dried pirfenidone and showed that at pharmacologically effective doses pulmonary delivery resulted in a 600-fold lower systemic exposure than oral doses in rat. In continuation of the work, Onoue *et al.* (30) showed that drug exposure in skin and eyes was 90-130-fold less in pulmonary than in oral administration. Along with the success of inhaled corticosteroids in asthma treatment this suggests that the harm-benefit-

profile of antifibrotics can be improved through pulmonary administration, which could be beneficial also when considering combination therapy in the treatment of IPF.

In this study, we show that an efficient antifibrotic effect can be achieved using a TGF-β/BMP modulating small molecule, tilorone, by using local administration in a well-established mouse model of pulmonary fibrosis. However, systemic dosing resulted in less fibrosis in histological analysis, as well as significantly lower collagen expression and anti-inflammatory effect, which was not seen in local administration. Better treatment results of systemic dosing can be explained by the measured drug concentration at the site of action as the measured lung tissue concentration in the pulmonary administration group was only approximately 2.5% of the concentration of the systemic group. As the local dose was 10% of the systemic dose, the difference in concentration is higher than would be expected from the difference in doses alone suggesting that either the delivery by aspiration is incomplete or the drug was cleared before penetrating the pulmonary epithelium. It is likely that even though the swallowing of the mice was prevented by holding the tongue during drug administration, a portion of the dose remained outside the airways e.g. in pharynx and was swallowed afterwards. Unfortunately, we were unable to determine blood concentration of tilorone due to technical difficulties, but Golovenko and Borisyuk (11) reported that there was no apparent accumulation of tilorone in lung tissue when compared to blood concentration in peroral administration. To the authors' knowledge, there have been no studies on the pharmacokinetics of tilorone in pulmonary administration. Determination of the optimal dosing and further development of the formulation, e.g. by adding permeation enhancers, could yield significant improvements in treatment results.

In conclusion, the data presented here shows that tilorone can be formulated to a reliable and well performing inhalable dry powder. We have shown that the powder retains its biological

activity despite the high reactor temperature, and that our formulation promotes more consistent permeation through a lung cell monolayer. Furthermore, the results from *in vivo* studies show that tilorone is a promising antifibrotic agent in both systemic and pulmonary administration.

Acknowledgements

The authors would like to thank Emma Paasikivi and Veronika Rezov for excellent technical assistance. We also thank Helena Taskinen (Tissue preparation and histochemistry unit at the Department of Anatomy, University of Helsinki) for paraffin sections and HE stainings. The provision of facilities by Aalto University at OtaNano - Nanomicroscopy Center (Aalto-NMC) is acknowledged. This study was funded by the Orion research foundation, the Finnish Medical foundation, the Sigrid Jusélius foundation, the Emil Aaltonen foundation, the Academy of Finland, the Finnish Cultural foundation, and the Jane and Aatos Erkko foundation. These funding bodies had no role in the design of the study, collection, analysis or interpretation of data, or in writing the manuscript.

Disclosures

The authors declare no conflicts of interest.

Author contributions

VV, MM, KK, JR, JTB, EK and LMB conceived and designed research; VV, LMB, NU, JV, EJ and ES performed experiments; VV, MM, KK, LMB and JR analyzed data; VV, MM, KK, LMB and JR interpreted results of experiments; VV and LMB prepared figures; VV drafted manuscript; VV, MM,

KK, LMB, JV, JTB and JR edited and revised manuscript; all authors approved final version of manuscript

References

1. **Barnes PJ**. Inhaled corticosteroids. *Pharmaceuticals* 3: 514–540, 2010.
2. **Bartram U**, **Speer CP**. The role of transforming growth factor beta in lung development and disease. [Online]. *Chest* 125: 754–65, 2004. http://www.ncbi.nlm.nih.gov/pubmed/14769761.
3. **Chaudhuri N**, **Duck A**, **Frank R**, **Holme J**, **Leonard C**. Real world experiences: Pirfenidone is well tolerated in patients with idiopathic pulmonary fibrosis. *Respir Med* 108: 224–226, 2014.
4. **Chono S**, **Fukuchi R**, **Seki T**, **Morimoto K**. Aerosolized liposomes with dipalmitoyl phosphatidylcholine enhance pulmonary insulin delivery. *J Control Release* 137: 104–109, 2009.
5. **Conte E**, **Gili E**, **Fagone E**, **Fruciano M**, **Iemmolo M**, **Vancheri C**. Effect of pirfenidone on proliferation, TGF-β-induced myofibroblast differentiation and fibrogenic activity of primary human lung fibroblasts. *Eur J Pharm Sci* 58: 13–9, 2014.
6. **Cottin V**, **Maher T**. Long-term clinical and real-world experience with pirfenidone in the treatment of idiopathic pulmonary fibrosis. *Eur Respir Rev* 24: 58–64, 2015.
7. **Denora N**, **Lopedota A**, **Perrone M**, **Laquintana V**, **Iacobazzi RM**, **Milella A**, **Fanizza E**, **Depalo N**, **Cutrignelli A**, **Lopalco A**, **Franco M**. Spray-dried mucoadhesives for intravesical drug delivery using N-acetylcysteine- and glutathione-glycol chitosan conjugates. *Acta Biomater* 43: 170–184, 2016.
8. **Eerikäinen H**, **Watanabe W**, **Kauppinen EI**, **Ahonen PP**. Aerosol flow reactor method for synthesis of drug nanoparticles. *Eur J Pharm Biopharm* 55: 357–360, 2003.
9. **Giron DJ**, **Schmidt JP**, **Pindak FF**. Tilorone hydrochloride: lack of correlation between interferon induction and viral protection. [Online]. *Antimicrob Agents Chemother* 1: 78–9, 1972. http://www.ncbi.nlm.nih.gov/pubmed/4670433.
10. **Gliński J**, **Chavepeyer G**, **Platten J-K**. Surface properties of aqueous solutions of l-leucine. *Biophys*

Chem 84: 99–103, 2000.

11. **Golovenko NY**, **Borisyuk IY**. Pharmacokinetics of amixin after repeated peroral administration to mice. *Bull Exp Biol Med* 140: 708–710, 2005.

12. **Gong L**, **Li D**. Preparation of novel pirfenidone microspheres for lung-targeted delivery: in vitro and in vivo study. *Drug Des Devel Ther* Volume 10: 2815–2821, 2016.

13. **Grainger CI**, **Greenwell LL**, **Lockley DJ**, **Martin GP**, **Forbes B**. Culture of Calu-3 cells at the air interface provides a representative model of the airway epithelial barrier. *Pharm Res* 23: 1482–1490, 2006.

14. **Haghi M**, **Young PM**, **Traini D**, **Jaiswal R**, **Gong J**, **Bebawy M**. Time- and passage-dependent characteristics of a Calu-3 respiratory epithelial cell model. *Drug Dev Ind Pharm* 36: 1207–1214, 2010.

15. **Hillamo RE**, **Kauppinen EI**. On the Performance of the Berner Low Pressure Impactor. *Aerosol Sci. Technol.* 14: 33–47, 1991.

16. **Hughes G**, **Toellner H**, **Morris H**, **Leonard C**, **Chaudhuri N**. Real World Experiences: Pirfenidone and Nintedanib are Effective and Well Tolerated Treatments for Idiopathic Pulmonary Fibrosis. *J Clin Med* 5: 78, 2016.

17. **Kauppinen E**, **Kurkela J**, **Brown D**, **Jokiniemi J**, **Mattila T**. Method and apparatus for studying aerosol sources [Online]. Google Patents: 2002. http://www.google.com.au/patents/WO2002059574A1?cl=en.

18. **King TE**, **Bradford WZ**, **Castro-Bernardini S**, **Fagan EA**, **Glaspole I**, **Glassberg MK**, **Gorina E**, **Hopkins PM**, **Kardatzke D**, **Lancaster L**, **Lederer DJ**, **Nathan SD**, **Pereira CA**, **Sahn SA**, **Sussman R**, **Swigris JJ**, **Noble PW**. A Phase 3 Trial of Pirfenidone in Patients with Idiopathic Pulmonary Fibrosis. *N Engl J Med* 370: 2083–2092, 2014.

19. **Koli K**, **Myllärniemi M**, **Vuorinen K**, **Salmenkivi K**, **Ryynänen MJ**, **Kinnula VL**, **Keski-Oja J**. Bone morphogenetic protein-4 inhibitor gremlin is overexpressed in idiopathic pulmonary fibrosis. *Am J Pathol* 169: 61–71, 2006.

20. **Kurkela JA**, **Kauppinen EI**, **Brown DP**, **Jokiniemi JK**, **Muttonen E**. A New Method and Apparatus

for Studying Performance of Inhalers. *Respir. Drug Deliv. VIII*. .

21. **Laaksonen T**, **Liu P**, **Rahikkala A**, **Peltonen L**, **Kauppinen EI**, **Hirvonen J**, **Järvinen K**, **Raula J**. Intact nanoparticulate indomethacin in fast-dissolving carrier particles by combined wet milling and aerosol flow reactor methods. *Pharm Res* 28: 2403–2411, 2011.

22. **Lakatos HF**, **Burgess HA**, **Thatcher TH**, **Redonnet MR**, **Hernady E**, **Williams JP**, **Sime PJ**. Oropharyngeal Aspiration of a Silica Suspension Produces a Superior Model of Silicosis in the Mouse When Compared To Intratracheal Instillation. *Exp Lung Res* 32: 181–199, 2006.

23. **Leppäranta O**, **Tikkanen JM**, **Bespalov MM**, **Koli K**, **Myllärniemi M**. Bone Morphogenetic Protein–Inducer Tilorone Identified by High-Throughput Screening Is Antifibrotic In Vivo. *Am J Respir Cell Mol Biol* 48: 448–455, 2013.

24. **Li RX**, **Yiu WH**, **Tang SCW**. Role of bone morphogenetic protein-7 in renal fibrosis. *Front Physiol* 6: 1–9, 2015.

25. **Lin X**, **Yu M**, **Wu K**, **Yuan H**, **Zhong H**. Effects of pirfenidone on proliferation, migration, and collagen contraction of human Tenon's fibroblasts in vitro. *Invest Ophthalmol Vis Sci* 50: 3763–70, 2009.

26. **Lähde A**, **Raula J**, **Kauppinen EI**. Simultaneous synthesis and coating of salbutamol sulphate nanoparticles with l-leucine in the gas phase. *Int J Pharm* 358: 256–262, 2008.

27. **Matubayasi N**, **Miyamoto H**, **Namihira J**, **Yano K**, **Tanaka T**. Thermodynamic quantities of surface formation of aqueous electrolyte solutions. V. Aqueous solutions of aliphatic amino acids. *J Colloid Interface Sci* 250: 431–7, 2002.

28. **Meyer K**, **Zimmermann I**. Effect of glidants in binary powder mixtures. *Powder Technol* 139: 40–54, 2004.

29. **Myllärniemi M**, **Lindholm P**, **Ryynänen MJ**, **Kliment CR**, **Salmenkivi K**, **Keski-Oja J**, **Kinnula VL**, **Oury TD**, **Koli K**. Gremlin-mediated decrease in bone morphogenetic protein signaling promotes pulmonary fibrosis. *Am J Respir Crit Care Med* 177: 321–9, 2008.

30. **Onoue S**, **Seto Y**, **Kato M**, **Aoki Y**, **Kojo Y**, **Yamada S**. Inhalable Powder Formulation of Pirfenidone with Reduced Phototoxic Risk for Treatment of Pulmonary Fibrosis. *Pharm Res* 30: 1586–1596, 2013.

31. **Ourique AF**, **Chaves P dos S**, **Souto GD**, **Pohlmann AR**, **Guterres SS**, **Beck RCR**. Redispersible liposomal-N-acetylcysteine powder for pulmonary administration: Development, in vitro characterization and antioxidant activity. *Eur J Pharm Sci* 65: 174–182, 2014.

32. **Paajanen M**, **Katainen J**, **Raula J**, **Kauppinen EI**, **Lahtinen J**. Direct evidence on reduced adhesion of Salbutamol sulphate particles due to L-leucine coating. *Powder Technol* 192: 6–11, 2009.

33. **Raula J**, **Kuivanen A**, **Lähde A**, **Kauppinen EI**. Gas-phase synthesis of l-leucine-coated micrometer-sized salbutamol sulphate and sodium chloride particles. *Powder Technol* 187: 289–297, 2008.

34. **Raula J**, **Lähde A**, **Kauppinen EI**. Aerosolization behavior of carrier-free l-leucine coated salbutamol sulphate powders. *Int J Pharm* 365: 18–25, 2009.

35. **Raula J**, **Rahikkala A**, **Halkola T**, **Pessi J**, **Peltonen L**, **Hirvonen J**, **Järvinen K**, **Laaksonen T**, **Kauppinen EI**. Coated particle assemblies for the concomitant pulmonary administration of budesonide and salbutamol sulphate. *Int J Pharm* 441: 248–254, 2013.

36. **Raula J**, **Thielmann F**, **Kansikas J**, **Hietala S**, **Annala M**, **Seppälä J**, **Lähde A**, **Kauppinen EI**. Investigations on the humidity-induced transformations of salbutamol sulphate particles coated with L-leucine. *Pharm Res* 25: 2250–2261, 2008.

37. **Richeldi L**, **du Bois RM**, **Raghu G**, **Azuma A**, **Brown KK**, **Costabel U**, **Cottin V**, **Flaherty KR**, **Hansell DM**, **Inoue Y**, **Kim DS**, **Kolb M**, **Nicholson AG**, **Noble PW**, **Selman M**, **Taniguchi H**, **Brun M**, **Le Maulf F**, **Girard M**, **Stowasser S**, **Schlenker-Herceg R**, **Disse B**, **Collard HR**. Efficacy and Safety of Nintedanib in Idiopathic Pulmonary Fibrosis. *N Engl J Med* 370: 2071–2082, 2014.

38. **Seto Y**, **Suzuki G**, **Leung SSY**, **Chan H-K**, **Onoue S**. Development of an Improved Inhalable Powder Formulation of Pirfenidone by Spray-Drying: In Vitro Characterization and Pharmacokinetic Profiling. *Pharm Res* 33: 1447–1455, 2016.

39. **Stringfellow DA**, **Glasgow LA**. Tilorone Hydrochloride: an Oral Interferon-Inducing Agent. *Antimicrob. Agents Chemother.* 2: 73–78, 1972.

40. **Vartiainen V**, **Bimbo LM**, **Hirvonen J**, **Kauppinen EI**, **Raula J**. Aerosolization, Drug Permeation and Cellular Interaction of Dry Powder Pulmonary Formulations of Corticosteroids with Hydroxypropyl-β-

Cyclodextrin as a Solubilizer. *Pharm Res* 56: 1–11, 2016.

41. **Vartiainen V**, **Bimbo LM**, **Hirvonen J**, **Kauppinen EI**, **Raula J**. Drug permeation and cellular interaction of amino acid-coated drug combination powders for pulmonary delivery. *Int J Pharm* 504: 89–97, 2016.

42. **Williams RO**, **Carvalho TC**, **Peters JI**. Influence of particle size on regional lung deposition - What evidence is there? *Int J Pharm* 406: 1–10, 2011.

43. **Xu Y**, **Meng H**. Pirfenidone-loaded liposomes for lung targeting: preparation and in vitro/in vivo evaluation. *Drug Des. Devel. Ther.* (June 2015). doi: 10.2147/DDDT.S84046.

44. **Zhang X**, **Yang L**, **Zhai S**, **Duan J**. Simultaneous quantification of tiloronoxim and tilorone in human urine by liquid chromatography–tandem mass spectrometry. *J Chromatogr B* 875: 349–357, 2008.

45. **Zhu Y**, **Lee KW**. Experimental study on small cyclones operating at high flowrates. *J Aerosol Sci* 30: 1303–1315, 1999.

Figure Captions

Figure 1. Scanning electron micrograph of leucine coated tilorone particles. Leucine forms rough crystalline surface on the drug particles.

Figure 2. Effect of tilorone on TGF-β(A) and BMP (B) signaling pathways. Tilorone was shown to inhibit TGF-βand induce BMP pathway in a concentration dependent manner. No statistically significant difference was seen between unprocessed and formulated drug. The results are expressed on a relative scale where the negative control was set to have the value 1. Reported values are averages of three independent experiments and the error bars represent the standard error of mean (SE). The data

were analyzed for statistical significance with nonparametric Mann-Whitney test. Asterisk indicates statistically significant ($p < 0.05$) difference compared to negative control.

Figure 3. Drug permeation across a differentiated Calu-3 cell monolayer. There was no statistically significant difference between formulated and unprocessed tilorone powder in drug permeation profiles. Results are averages of four independent experiments and the error bars represent the standard error of mean (SE). To compare individual data points a multiple t-test followed by a Holm-Šídák correction test (significance level, alpha, set to 5%) was used.

Figure 4 Histological analysis of mouse lung tissue. Representative images of hematoxylin and eosin stained tissue from non-treated control group (A, non-treated), silica-exposed control group (B, SiO_2-Ctrl), systemic treatment group (C, SiO_2-Systemic) and local treatment group (D, SiO_2-Local) are shown. Systemic administration of tilorone resulted in a decrease of histological scoring for both fibrosis and inflammation when compared to SiO_2-Ctrl group. Local dosing resulted in a decrease in the histological scoring of fibrosis. Mean value is reported for each group (n=12). The error bars represent the standard error of mean (SE). The data were analyzed for statistical significance with nonparametric Mann-Whitney test. Asterisk indicates statistically significant ($p < 0.05$) difference compared to SiO_2-Ctrl group.

Figure 5. **Type I collagen** (*Col1a1*) mRNA expression. Silica exposure increased the expression in exposed controls (SiO_2-Ctrl). Systemic administration resulted in a significant decrease of **type I collagen** expression. Mean value is reported for each group (n=12) and the error bars represent the standard error of mean (SE). The data were analyzed for statistical significance with nonparametric

590 Mann-Whitney test. Asterisk indicates statistically significant ($p < 0.05$) difference compared to SiO_2-Ctrl group.

Tables

Table 1: Aerosolization results of the carrier-free fine powders formulation

	ED (mg)	CV (%)	FPF (%)	MMAD (µm)	GSD (µm)	ED_eff (%)
2 kPa EH	3.0	9	28	3.3	1.7	
4 kPa EH	3.0	8	30	3.8	1.7	
2 kPa Tw	4.8	7	22	3.4	1.7	95
4 kPa Tw	4.1	11	33	3.2	1.7	81

595

Actuation from Easyhaler (EH) and Twister (Tw) at two pressure drops and inhalation flow rates. For 600 Easyhaler 2 kPa = 43 L/min and 4 kPa = 55L/min, and for Twister 2 kPa = 40 L/min and 4 kPa = 55 L/min. ED is average emitted dose (n=10); CV is coefficient of variation of emitted dose; FPF is fine particle fraction (geometric mean diameter <5µm); MMAD is mass median aerodynamic diameter; GSD is geometric standard deviation; ED_{eff} is the emptying efficiency of powder from Twister

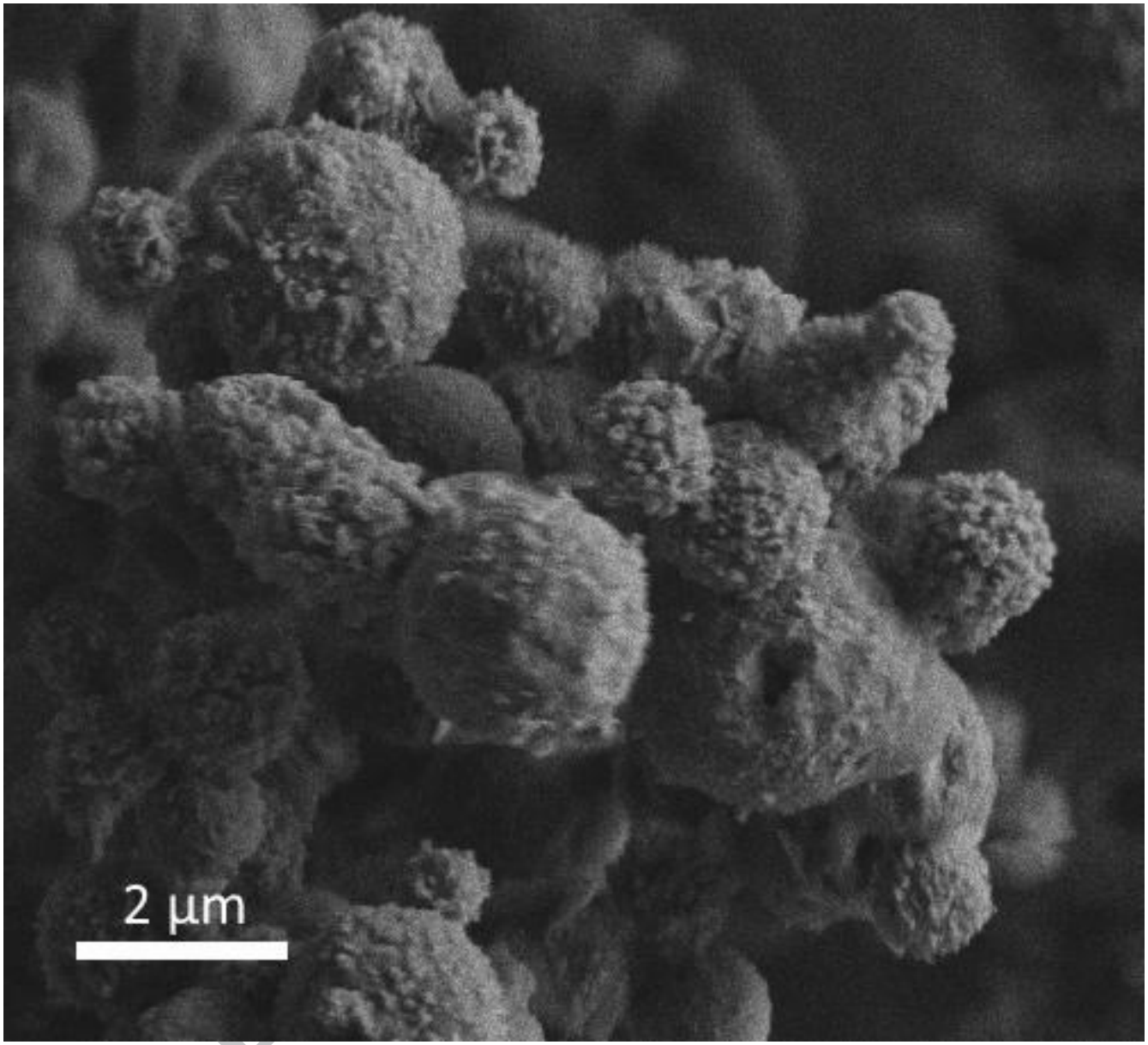

605

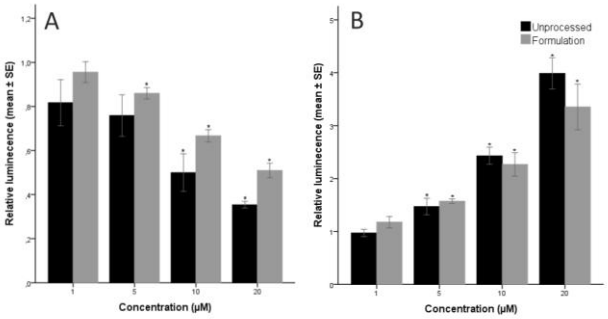

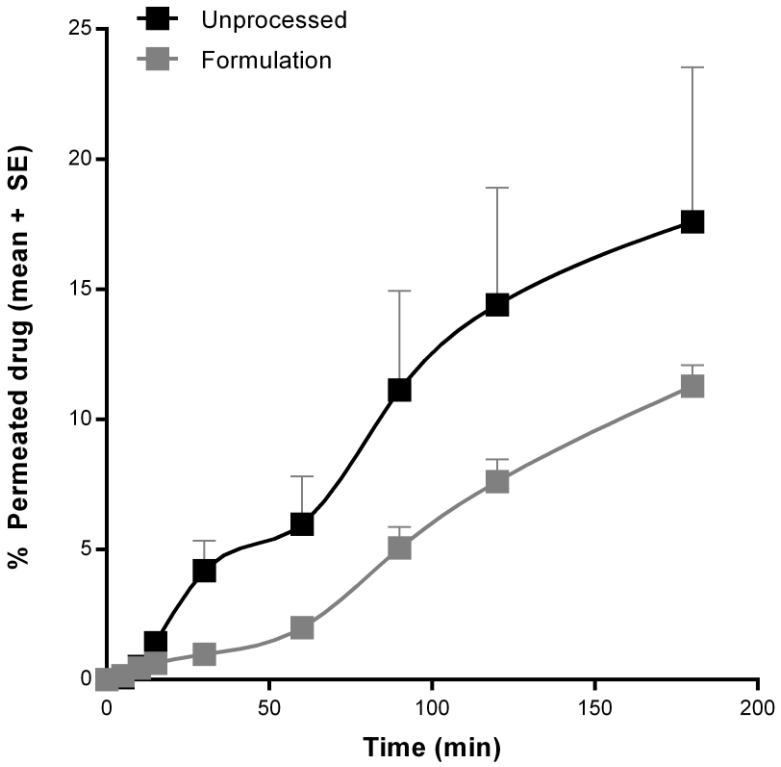

610

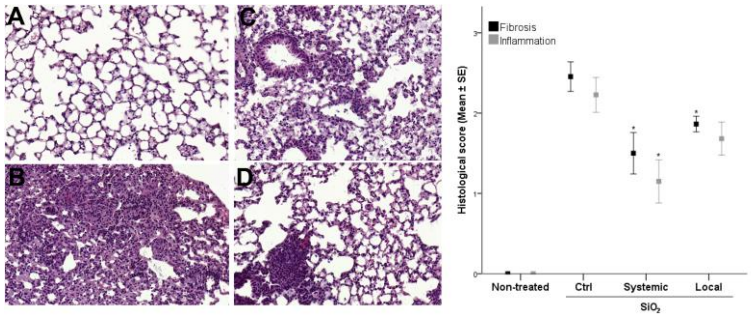

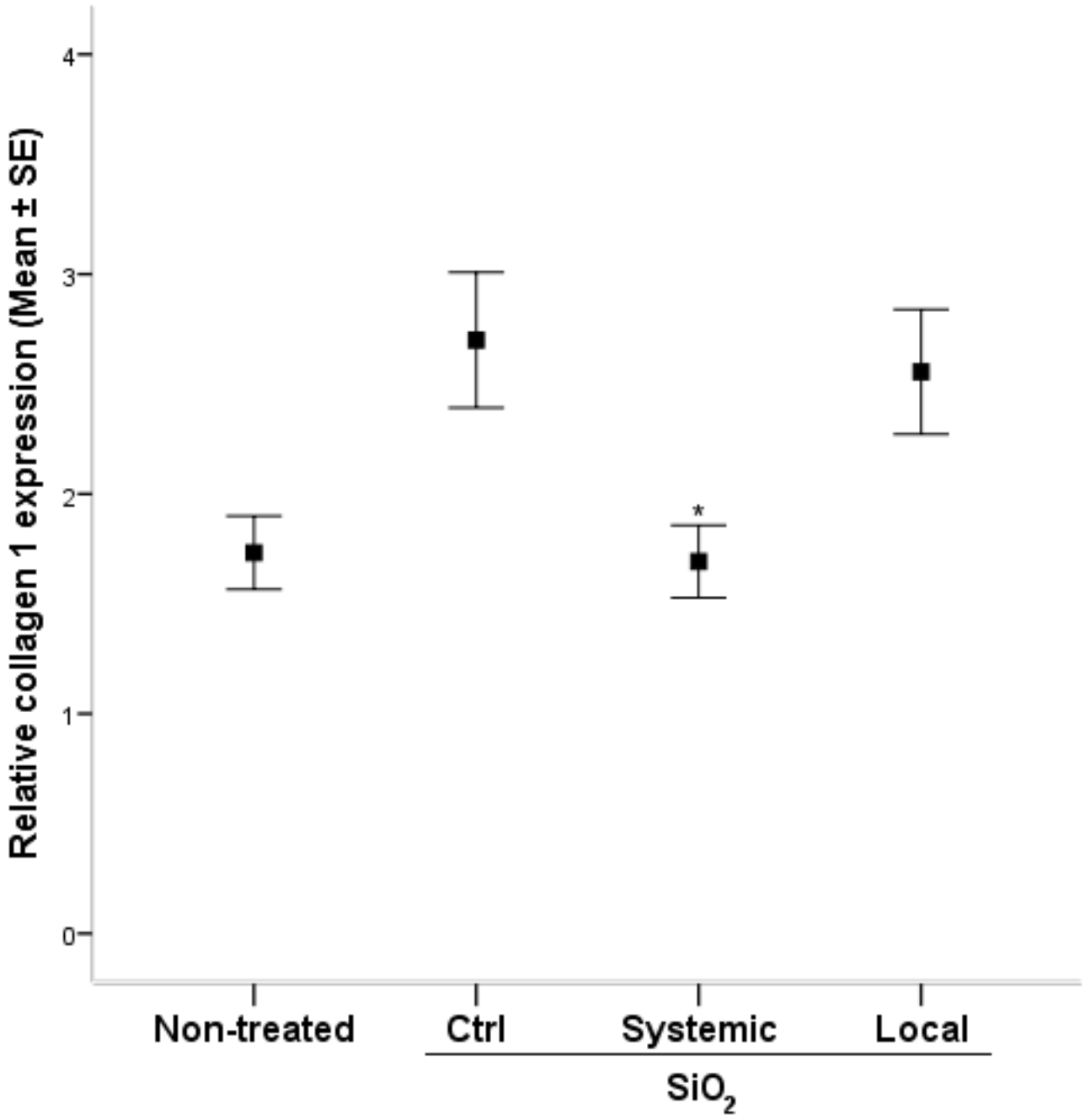
Relative collagen 1 expression (Mean ± SE)
4
3
2
1
0
*
Non-treated
Ctrl
Systemic
Local
SiO2

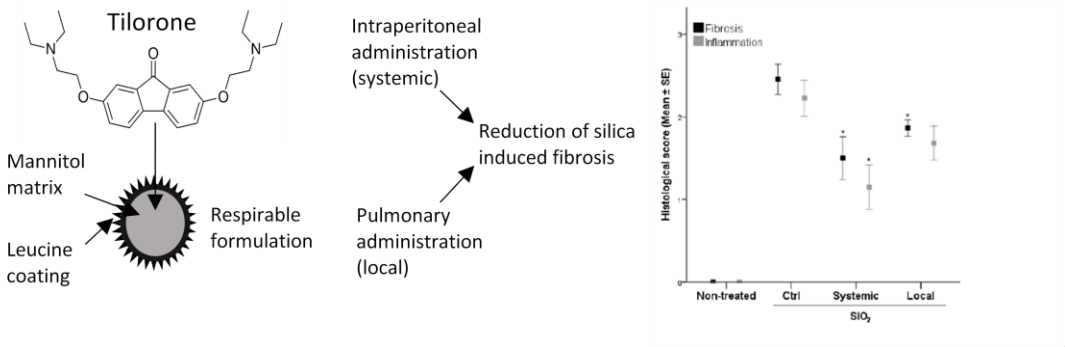

615